Experimental and theoretical investigation of scattering from a distribution of cracks

Jerrol W. Littles, Jr.*, Laurence J. Jacobs* and Jianmin Qu†

*School of Civil Engineering, Engineering Science and Mechanics Program, Georgia Institute of Technology, Atlanta, GA 30332-355, USA
†G.W. Woodruff School of Mechanical Engineering, Georgia Institute of Technology, Atlanta, GA 30332-405, USA

Received 20 October 1993; revised 20 September 1994

This paper presents the results of an experimental and theoretical investigation that studies the scattering of longitudinal elastic waves by a distribution of cracks. The experimental portion measures the transmission coefficients at imperfect interfaces using a high fidelity heterodyne interferometer. Specimens are manufactured with known distributions of cracks that vary from 0% (perfect interface) to 24%. Incident longitudinal elastic waves are generated with a broadband, contact piezoelectric transducer and the backscattered wave field is measured with the interferometer. The theoretical analysis examines the interaction of elastic waves with a distribution of cracks using a differential self-consistent scheme in conjunction with Auld's formula for backscattering. In this model the multiple scattering problem from a distribution of cracks is reduced to finding the crack opening displacement of a single crack. Transmission coefficients are presented as functions of incident wave-number, flaw size and percentage of defects. The experimentally measured values are compared with the theoretically predicted results and excellent agreement is obtained.

Keywords: non-destructive evaluation; ultrasonic inspection; laser interferometry; transmission coefficients; differential self-consistent scheme

Ultrasonic inspection is an established non-destructive evaluation method for detecting defects in structural components; this technique examines the interaction of elastic waves with flaws to determine the size and location of the flaws. Of particular interest is the ability to detect defects in an interface between two materials. An incident elastic wave that interacts with an interface between two materials will create both reflected and transmitted waves that propagate away from the interface. For a perfect interface, the amount of the incident wave that is transmitted and reflected is only dependent upon the material properties of the two media; the resulting waves are independent of the frequency content of the incident waveform. The solution for the coefficients of the transmitted and reflected waves, as a function of the incident wave coefficient and the material properties, is available in a number of sources, such as Reference 1. However, if the interface is not perfect, the interaction between the incident, reflected and transmitted waves is more complicated. This paper presents the results of both an experimental and theoretical analysis of the effect of a distribution of cracks on the reflected and transmitted waves. In this study, the distribution of cracks exists in an interface between the same material. The experimental results are used both to observe specific experimental trends, such as the effect of incident wave frequency, and to validate the theoretical model. The objective of this work is to provide a quantitative study of the interaction of elastic waves with imperfect interfaces.

Because of the varied applications of this problem, the backscatter of elastic waves from a distribution of defects has been studied by numerous investigators using a variety of techniques. Ismagilov *et al.*[2] were concerned with the backscatter of longitudinal waves from thin plates randomly oriented in a liquid. Kawahara and Yamashita[3] studied the scattering of seismic waves from a 'fault zone' by employing a theoretical study of elastic waves due to a random distribution of cracks. Rao and Zhu[4] used a statistical approach to estimate the scatterer number density of a uniform material with randomly distributed scattering bodies. All of these papers are concerned with a random distribution of defects. Sotiropoulos and Achenbach[5] modelled an imperfect diffusion bond as a non-periodic distribution of cracks and calculated the transmission and reflection coefficients in terms of the number of cracks per unit length. The model was verified by comparison with exact results. Angel and Achenbach[6] calculated the reflection and transmission of longitudinal and transverse elastic waves due to an array of periodically distributed cracks of equal length. Fourier series expansions were used to reduce the mixed-boundary value problem to a singular integral equation of the first kind for the dislocation density along the crack faces.

SSDI 0041-624X(95)00037-7

The experimental procedure in this investigation uses a laser interferometer to measure the transmitted wave field in four Plexiglas specimens that contain different percentages of cracks. The high fidelity and non-contact nature of the interferometric measurements are critical for the success of this approach. Harmonic incident longitudinal waves are generated with a contact piezoelectric transducer driven by a function generator. The specimens are manufactured by bonding two Plexiglas blocks, one of which contains 'crack-like' defects. The bonds, which are made with Plexiglas cement, have identical material properties as the base Plexiglas. The resulting specimens contain a controlled distribution of defects that exist along an interface between two media with identical properties.

The theoretical procedure is based on a differential self-consistent scheme (DSCS)[7] together with Auld's backscattering formula[8]. First, the backscattered signal from an array of cracks is calculated using Auld's formula by treating the array as a uniform interphase. Next, the solution for the backscattering of a single crack in an effective interphase is determined. The DSCS states that the backscatterer from $N + 1$ cracks is equal to the sum of the backscatter from N cracks, plus the backscatter from a single crack in an effective interphase. This results in a first-order linear, ordinary differential equation that is solved in closed form. The theoretical results are compared with the experimentally obtained values and their accuracy and significance for non-destructive testing is discussed.

Experimental procedure

Specimens with defects of 0, 10, 20 and 24% are manufactured. The 0% specimen is a perfectly bonded sample and will be used in a normalization procedure to calculate the transmission coefficients. To ensure the consistency and accuracy of the final results, the same process is used to manufacture all of the samples. The number of cracks needed to produce the desired defect percentage is given as $N = CL/a$, where C is the density of crack distribution, N is the number of cracks in length $2L$ and $2a$ is the crack length. The specimens are manufactured using two pieces of 10.16 cm × 10.16 cm × 2.54 cm Plexiglas. Defects are manufactured by cutting a groove approximately 1 mm deep into the face of one of the Plexiglas samples with a band saw. The total length of the defect ($2a$) is also 1 mm. A stencil is used to ensure that the defects are evenly spaced along the face of the Plexiglas. Each specimen is made so that the centre line between the middle two defects is located at the centre of the specimen's face. This ensures a consistent method for spacing the defects of the various specimens, but limits the specimens to defect percentages which have an even number of cracks.

A thin coat of Plexiglas cement is applied to the surface of the Plexiglas and is used to bond both pieces together. A wax coated filament is placed in the saw cut defects in order to prevent them from being filled with cement during bonding. The two pieces are pressed together with a vice that applies a sufficient force to squeeze out any air bubbles that may have become trapped on the interface. In addition, this causes the Plexiglas cement bond to become extremely thin. The dried Plexiglas cement has the same physical properties as the original Plexiglas and consequently the boundary between the two pieces of Plexiglas has the same physical properties as any other point within the specimen. As a result, the interface bond is neglected and the specimens are treated as having one pair of material constants, λ and μ. Once the cement has dried, the specimen is heated, causing the wax to melt. The filament and molten wax are removed, leaving a thin, 'crack-like' defect. An additional benefit of using Plexiglas to manufacture the specimen is that the quality of the bond and the shape of the artificial cracks may be visually observed. The final specimens are 10.16 cm × 10.16 cm × 5.08 cm. These dimensions are such that reflections from the sides of the sample arrive (at the interferometric probe) after the entire original pulse has been sampled; the specimen geometry does not influence any of the measured waveforms.

The high fidelity laser interferometer that is used in this procedure is described in detail in Reference 9. Briefly, a single frequency laser light is split into two beams that are separated in frequency by 40 MHz using an acousto-optic modulator. These two beams are sent along two paths of the interferometer, one of which contains the sample being monitored. The two beams are recombined at a photodetector and produce a beat frequency of 40 MHz. Frequency shifts in light reflected from the sample surface result in proportional frequency shifts in the 40 MHz beat signal. As a result, this 40 MHz signal acts as a carrier that is demodulated in real time with an FM discriminator to obtain the time-dependent surface velocity. The interferometer makes high-fidelity, absolute measurements of surface velocity over a bandwidth of 10 MHz. Since this type of measurement does not touch or acoustically load the specimen, the event being observed is undisturbed by the measurement process. Waveforms are recorded on a digital oscilloscope and transferred to a personal computer via a GPIB interface.

The experimental set-up consists of a specimen, alignment fixture, broadband contact piezoelectric transducer, function generator and the heterodyne interferometer. The specimen is placed in the alignment apparatus and the piezoelectric transducer is pressed against the back of the specimen by a threaded rod. The alignment fixture is used to consistently align the transducer, specimen and interferometer; this consistency is critical for the proposed normalization procedure. Any variation is removed by centring the transducer on the threaded rod, thus orientating the transducer and interferometric probe in exactly the same locations for each test. In addition, consistent couplant thickness and transducer pressure is also important for the repeatability of the experiments. The threaded rod that is used to press the transducer against the surface of the specimen is tightened the same amount for each test, thus producing the same pressure and couplant thickness. This procedure, combined with the accuracy of the interferometer, produces a typical variation of under 4% when a specimen is removed and the entire test is repeated.

Once proper transducer/interferometer alignment is obtained, a function generator is used to excite the transducer and create the incident longitudinal wave. The transducer is excited with a two-cycle harmonic burst over a range of frequencies that are prescribed by the function generator. For each specimen, incident waves

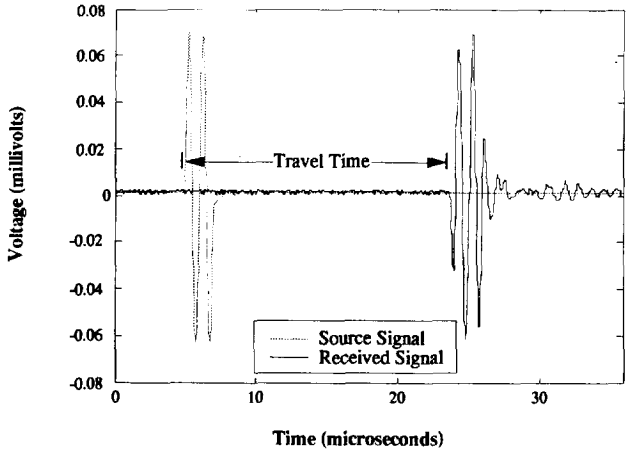

Figure 1 Typical source signal and response signal

are generated at 16 discrete harmonic frequencies that vary from 0.25 MHz to 1.5 MHz. The peak-to-peak voltage of the driving signal from the function generator is kept at a constant value of 25 V throughout the frequency range. The resulting surface velocities (that are measured with the interferometer) are averaged, using a digital oscilloscope, over 200 separate input signals for each individual frequency. This signal averaging procedure significantly increases the signal-to-noise ratio. A typical averaged signal and its corresponding input signal are shown in *Figure 1*; this figure shows that the magnitude of the 'noise' is insignificant when compared with the actual signal. The 'travel time' indicated in *Figure 1* is the amount of time that it takes for the longitudinal elastic wave to travel through the 5.08 cm thickness of the specimen; in this case, 18.6 μs. This time is used to calculate the longitudinal wave speed, 2731 m s^{-1}, which compares quite well with the published value of 2700 m s^{-1} in Plexiglas.

In addition, spatial averaging is used to obtain an accurate representation of the scattering effects; measurements are made at a number of spatial locations and these results are averaged. This reduces local effects that can occur due to the point detection nature of the interferometer. This averaging is especially important for the higher percentage defect specimens. For example, the results presented for the 24% specimen represent the average of five spatial locations.

Experimental results

An effective measure of the magnitude of each experimentally measured signal is the magnitude from the first major crest to the first major trough. This peak-to-peak value, referred to as Δ (see *Figure 2*), is a measure of the transmission coefficient for each discrete driving frequency. It is important to note the absolute nature of the interferometric measurements; the vertical axis of *Figure 2* shows the surface velocity in mm s^{-1}. Although the transducer used to generate the incident elastic waves is broadband, its actual output is not constant over the range of frequencies considered in this study. The 0% defect specimen provides a representation of the transducer's flatness over the desired frequency range. *Figure 3* shows the peak-to-peak amplitudes (in terms of surface velocities), Δ, versus the input frequency for all four specimens. These surface velocity data are used to calculate the transmission coefficients, as functions of frequency, for each specimen.

The transmission coefficients are calculated by dividing the peak-to-peak amplitude, Δ, for a particular specimen by the peak-to-peak amplitude of the 0% defect specimen at each corresponding frequency. This calculation gives the amount of the incident signal transmitted through each block, as a function of frequency, normalized to the 0% defect specimen. This normalization to the 0% specimen is necessary since the coefficient of the incident wave is unknown. It is important to note that the peak-to-peak amplitudes measured in the 0% specimen are functions of the transducer type and pressure, couplant thickness, driving frequency and voltage, as well as any propagation losses (such as attenuation) that occur in this perfectly bonded specimen. In contrast, the peak-to-peak amplitudes in the 10, 20 and 24% specimens contain all of these effects as well as any scattering losses due to the presence of the defects. This normalization of the 10, 20 and 24% amplitudes (Δs) to the 0% amplitudes (Δs) removes the influence of any propagation losses and transducer related features, leaving only the effect of the scattering due to the array of cracks. It is important to note that since the

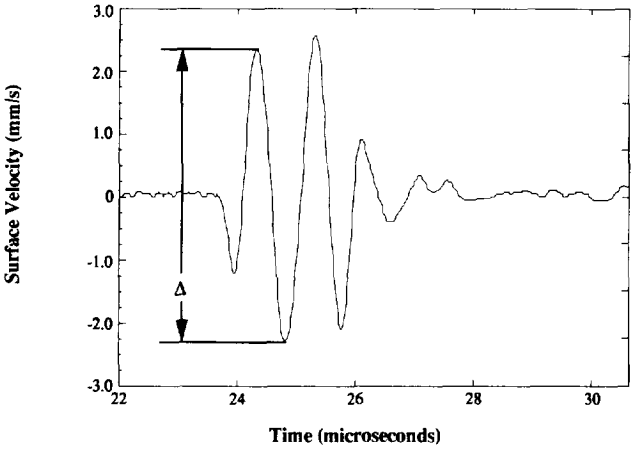

Figure 2 Typical surface velocity versus time signal

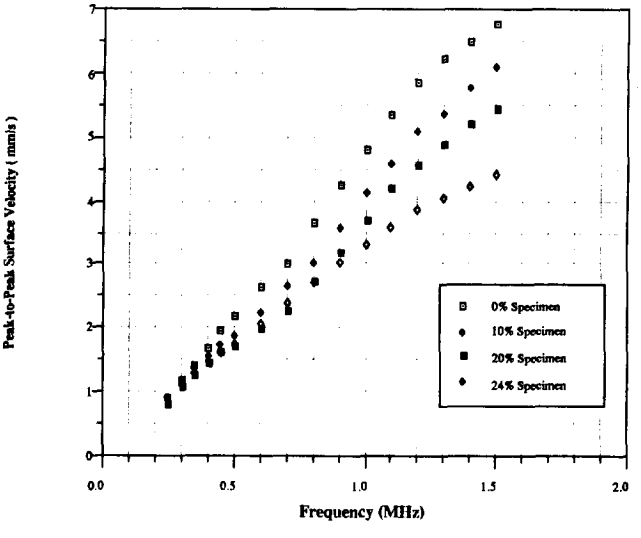

Figure 3 Peak-to-peak surface velocity, Δ, versus frequency

interferometer is broadband and non-contact, it does not influence the measured waveforms.

The transmission coefficients for each specimen are plotted versus the dimensionless frequency, $k_T a$ in *Figures 4–6*. Here, k_T is the transverse wave-number (frequency divided by transverse wave speed) and a is one half of the crack length. These figures contain the discrete transmission coefficients for each of the 16 experimentally measured frequencies, as well as a continuous curve. The

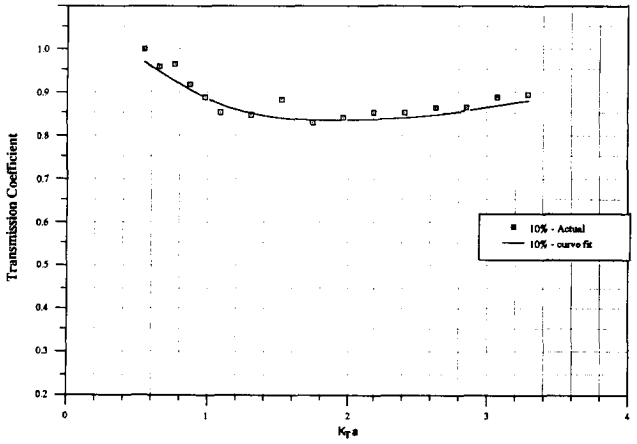

Figure 4 Experimental transmission coefficient versus $k_T a$, 10% specimen

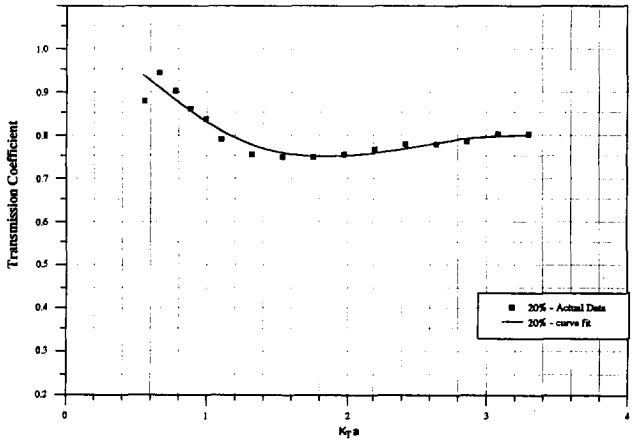

Figure 5 Experimental transmission coefficient versus $k_T a$, 20% specimen

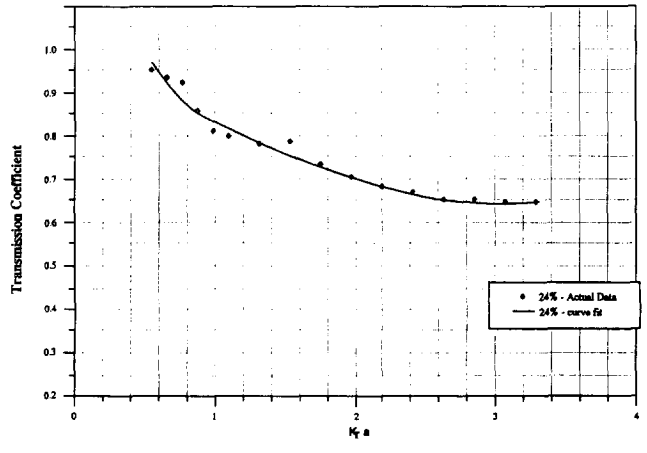

Figure 6 Experimental transmission coefficient versus $k_T a$, 24% specimen

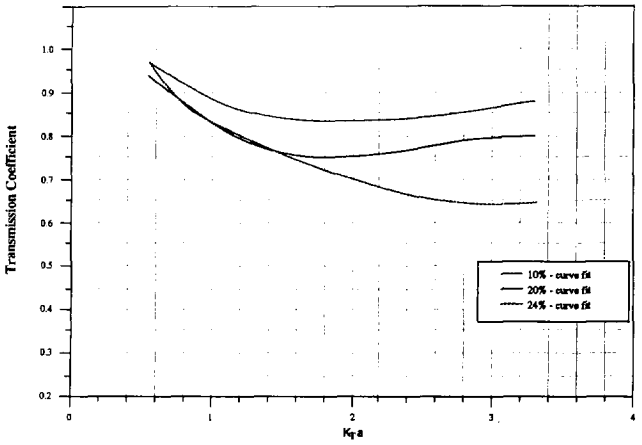

Figure 7 Comparison of experimental transmission coefficients

curves represent a fourth-order fit to the individual data points. The curves model the broadband transmission response, based on the 16 discrete, harmonic waveforms. It should be noted that the fitted curves are only used to help visualize the data; they make it easier to observe experimental trends. The standard deviation of the discrete values from the curve fit is calculated for each plot. The standard deviations are 1.89, 2.07 and 1.64 for the 10%, 20% and 24% defect specimens, respectively. *Figure 7* is a comparison of the transmission coefficients for each of the three specimens.

In general, the 10 and 20% specimens show consistent results, while the values of the 24% sample do not agree as well. The experimental results show the expected trend of decreasing transmission coefficients for increasing percent defects. In other words, there is more scattering when there are more defects present, regardless of frequency. However, there is some discrepancy between the 20% and 24% samples for $k_T a$ values less than 1.5. The 10% and 20% samples show a sharp decrease in transmission for increasing $k_T a$, up to approximately 1.6. This decrease is followed by a flat region (zero slope) that leads to a gradual increase in transmission for increasing $k_T a$. The 24% specimen shows a longer portion of decreasing transmission for increasing $k_T a$ (up to 2.8) followed by a flat region and then a slight upward trend. These results show the complicated nature of this scattering problem; the transmission coefficients depend on the ratio of the crack length ($2a$), to incident wavelength, as well as the number of defects in the array.

It should be noted that it is difficult to manufacture specimens with high percentages of defects; the large number of artificial saw cuts seems to cause additional cracks and voids that form in the Plexiglas bond that are not accounted for in this analysis. In addition, the spatial averaging scheme needed to compensate for the point receiver nature of the interferometer becomes more critical for these higher percentage defect samples. All of these factors contribute to the anomalies shown in the 24% results.

Theoretical model

The theoretical model is used to evaluate the interaction of ultrasonic waves and a distribution of cracks along a material interphase. The model employs a differential

self-consistent scheme (DSCS) together with Auld's backscattering strength formula. Auld's formula is used to calculate the backscattering, or reflection, due to an interphase and a single crack in an effective interphase. The DSCS is then used to find the reflection coefficient, R, for any given percentage of defects (C). The DSCS calculates the reflection coefficient by determining the additional effect due to a single crack that is added to an array of cracks. The transmission coefficient, T, is then determined from the reflection coefficient. These transmission coefficients are then compared with the experimentally calculated values.

The theoretical model treats the problem as a distribution of cracks on the interphase of two half-spaces. A Cartesian coordinate system is used such that the interphase is located at $x_2 = 0$. An incident longitudinal wave is assumed to be propagating normal to the material interphase, in the positive x_2 direction, originating from $x_2 = -\infty$. The upper half-space is referred to as region 1; the lower half-space is referred to as region 2 (*Figure 8*). The size of a single crack is assumed to be small when compared with the incident wavelength. The material constants λ and μ, as well as the density, ρ, are assumed to be identical in both half-spaces. The displacement components far away from the distribution of cracks are written as

$$\begin{aligned} u_i &= e^{ik_L x_2} + Re^{-ik_L x_2} \qquad \text{for } x_2 < 0 \\ u_i &= Te^{ik_L x_2} \qquad \text{for } x_2 > 0 \end{aligned} \tag{1}$$

where R and T are the reflection and transmission coefficients discussed previously and k_L is the longitudinal wave-number. The time dependent term, $e^{i\omega t}$, is common to all the displacement terms and will be omitted throughout this manuscript for brevity.

Auld's Formula for backscattering is developed using a two-transducer, through-transmission system. Transducer 1 produces an incident field of power P, and transducer 2 is the receiver. The ratio of received electrical signal strength, E_{II}, to the incident electrical signal strength, E_I, is denoted by Γ. The change in the ratio, $\delta\Gamma$, due to a single flaw is given by Auld's formula

$$\delta\Gamma = [(E_{II})_{flaw} - (E_{II})_{noflaw}]/[(E_I)_{flaw}] \tag{2}$$

This formula may be simplified for the case of backscattering

$$\delta\Gamma = -\frac{i\omega}{4P}\int_S (\sigma_{kj}^{(2)}u_k^{(1)} - \sigma_{kj}^{(1)}u_k^{(2)})n_j \, dS \tag{3}$$

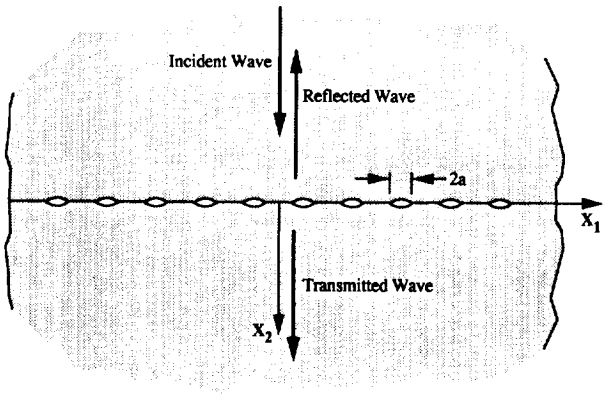

Figure 8 Interphase cracks with incident, reflected and transmitted waves

where S is an arbitrary surface which surrounds the scatterer and n_j is the unit outward normal of S. In Equation (3), the terms with superscript (1) relate to the fields in the absence of the scatterer, while terms with the superscript (2) relate to the fields in the presence of the scatterer. For the case where the scatterer is a traction free crack, Equation (3) is simplified to

$$\delta\Gamma = -\frac{i\omega}{4P}\int_{A+} (\sigma_{kl}^{(1)}\Delta u_k^{(2)})n_l \, dS \tag{4}$$

where A^+ is the crack area and

$$\Delta u_k^{(2)} = u_k^{(2)}(x_2^-) - u_k^{(2)}(x_2^+)$$

Equations (3) and (4) will be used to calculate the backscattering from an interphase and a single crack on an effective interphase.

If the array of cracks on the line $x_2 = 0$ is treated as an interphase, the total displacement field for $x_2 < 0$ is given by Equation (1). By treating the entire lower half-space as a scatterer, Auld's formula yields

$$\delta\Gamma = -\frac{i\omega}{4P}\int_{-\infty}^{+\infty} (\sigma_{22}^{(2)}u_2^{(1)} - \sigma_{22}^{(1)}u_2^{(2)})|_{x_2=0} \, dx_1 \tag{5}$$

where the solution in the absence of the scatterer (the incident field only) becomes

$$u_2^{(1)} = e^{ik_L x_2}$$

$$\sigma_{22}^{(1)} = ik_L(\lambda + 2\mu)e^{ik_L x_2}$$

and the solution in the presence of the scatterer (incident and reflected fields) may be expressed as

$$u_2^{(2)} = e^{ik_L x_2} + Re^{-ik_L x_2}$$

$$\sigma_{22}^{(2)} = ik_L(\lambda + 2\mu)e^{ik_L x_2} - ik_L(\lambda + 2\mu)Re^{-ik_L x_2}$$

Equation (5) is integrated from $-L$ to $+L$ (the specimen width) to obtain

$$\frac{4P}{i\omega}\delta\Gamma = 4i(\lambda + 2\mu)k_L RL \tag{6}$$

It is important to note that R is now a function of C, the percentage of defects.

Next, Auld's formula is evaluated for the case of a single crack on an effective interphase as

$$\delta\Gamma = -\frac{i\omega}{4P}\int_{-a}^{+a} (\sigma_{22}^{(1)}\Delta u_2^{(2)})|_{x_2=0} \, dx_1 \tag{7}$$

where the solution in the absence of the scatterer (the interphase without the crack) yields

$$\sigma_{22}^{(1)} = ik_L(\lambda + 2\mu)e^{ik_L x_2} - ik_L(\lambda + 2\mu)Re^{-ik_L x_2}$$

and the solution in the presence of the scatterer (both the single crack and interphase) becomes

$$\Delta u_2^{(2)} = (1 - R)\Delta u_2^S$$

where Δu_2^S is the crack opening displacement (COD) due to the incident wave, $e^{ik_L x_2}$. The evaluation of Equation (7) yields

$$\frac{4P}{i\omega}\delta\Gamma = iak_L(\lambda + 2\mu)(1 - R)^2 V \tag{8}$$

with

$$V = \int_{-1}^{+1} \Delta u_2^S(a\xi) \, d\xi \tag{9}$$

which must be evaluated numerically. In this paper, a boundary element method is used to calculate V numerically at a number of discrete frequencies.

The Differential Self-Consistent Scheme (DSCS) is based on the idea of constructing a backscattering model by adding the effect of one crack at a time. The procedure is based on the solution to the following three problems.

Problem 1 assumes that $N + 1$ cracks of length $2a$ are located on an interphase of length $2L$, giving a defect percentage of $C_1 = a(N + 1)/L$. The reflection coefficient from this effective interphase is given by $R(C_1)$. The backscattering due to this array of cracks is found from Equation (6) to be

$$\delta\Gamma(C_1) = \frac{i\omega}{4P}[4ik_L R(C_1)L(\lambda + 2\mu)] \tag{10}$$

Problem 2 treats an array of N cracks on a perfect interphase as a scatterer. In this case, the crack density on the interphase is $C = aN/(L - a)$. The reflection coefficient from this effective interphase is given by $R(C)$. The backscattering due to this array of cracks is obtained from Equation (6) as

$$\delta\Gamma(C) = \frac{i\omega}{4P}[4ik_L R(C)L(\lambda + 2\mu)] \tag{11}$$

Problem 3 assumes that a crack of length $2a$ is added to an interphase which has a crack density of $C = aN/(L - a)$ and a corresponding reflection coeffcient given by $R(C)$. As stated previously, the DSCS assumes that the scattering from $N + 1$ cracks may be found by adding the scattering of N cracks and the scattering of a single crack. From this, it is seen that the scattering from $N + 1$ cracks (Equation (10)) is equal to the addition of the scattering from N cracks (Equation (11)) and the scattering from a single crack (Equation (8)). That is

$$\delta\Gamma(C_1) = \delta\Gamma(C) + \frac{i\omega}{4P} iak_L(\lambda + 2\mu)(1 - R(C))^2 V \tag{12}$$

Substitution and simplification yields

$$\frac{dR}{dC} = \frac{V(1 - R)^2}{4(1 - C)} \tag{13}$$

Equation (13) is a first-order linear, ordinary differential equation with the initial condition of

$$R(0) = 0$$

That is, the reflection coefficient will be equal to zero for a specimen with no defects. Using this initial condition, Equation (13) is solved for the reflection coefficient, R, as

$$R = \frac{-V\ln(1 - C)}{4 - V\ln(1 - C)} \tag{14}$$

while the solution for the transmission coefficient is

$$T = 1 - R = \frac{4}{4 - V\ln(1 - C)} \tag{15}$$

It is important to note that although the theoretical model is developed for low crack densities, the solution is exact for very high crack densities. For example, in Equation (14) when the density C approaches 1 (no bond between the upper and lower half-spaces), the reflection coefficient R approaches 1 (total reflection).

Theoretical results and discussion

The theoretical model is evaluated over a range of frequencies corresponding to those examined in the experimental portion, and for values of crack densities of 10, 20 and 24%. A plot of the theoretical transmission coefficients versus $k_T a$ is shown in *Figure 9*, while *Figures 10–12* are comparisons between the theoretical and experimental transmission coefficients for each sample.

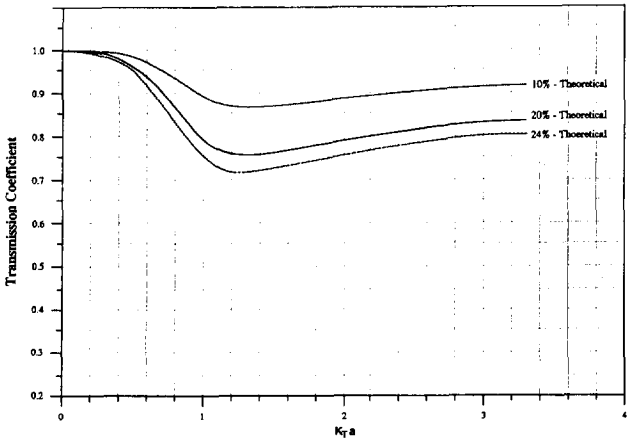

Figure 9 Comparison of theoretical transmission coefficients

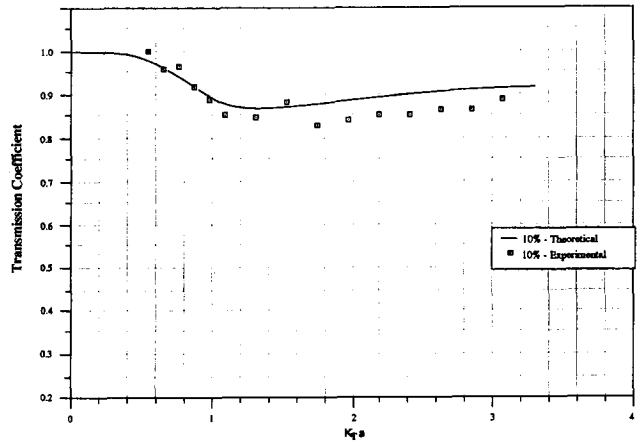

Figure 10 Theoretical and experimental transmission coefficients, 10% specimen

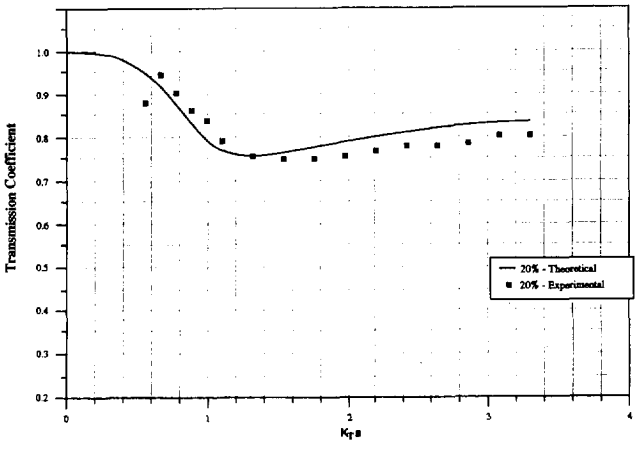

Figure 11 Theoretical and experimental transmission coefficients, 20% specimen

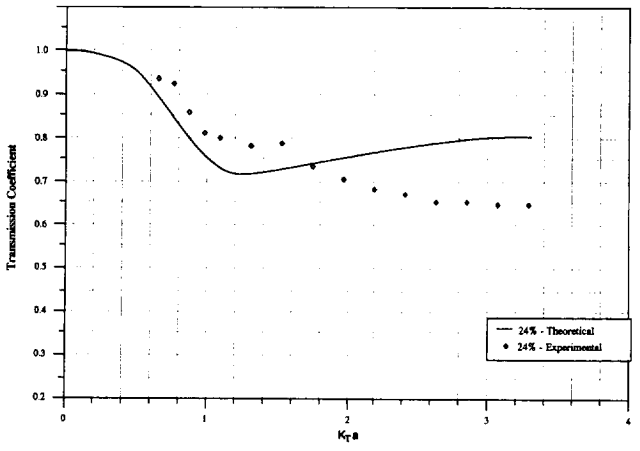

Figure 12 Theoretical and experimental transmission coefficients, 24% specimen

For conciseness, the experimental results are shown in terms of the discrete data points. The standard deviation of these experimental values from the theoretical curve is calculated for each plot. These standard deviations are 3.34, 3.66 and 8.62 for the 10, 20 and 24% defect specimens, respectively.

In general, there is excellent agreement between the theoretical and experimental results. For example, the maximum difference between theory and experiment for the 10% specimen is approximately 6%, while the similar value for the 20% sample is 4%. In addition, both the experimental and theoretical results show the same global trends of decreasing transmission, followed by a local minimum and finally increasing transmission. As expected, the 24% results are not as consistent, but still show the same global trends. The discrepancies of the 24% specimen are due to the difficulties encountered in manufacturing a 'true' 24% sample, as previously discussed. It is interesting to note that for higher frequencies ($k_T a$ greater than 1.6), the experimental results consistently predict more scattering than the theoretical model. This is due to limitations in the theoretical model; the theoretical approach is only valid for wavelengths much larger than the half crack length a. This assumption is violated in the higher frequency region of these curves.

Conclusions

This paper demonstrates the effectiveness of laser interferometric techniques for the experimental investigation of scattering by a distribution of cracks and verifies the accuracy of the differential self-consistent scheme. The experimentally measured values are compared with the theoretically predicted results and excellent agreement is obtained. This work shows that the transmitted waveform through an array of cracks is dependent upon the percentage of cracks, the size of each crack and the frequency of the incident wave.

These results are an important first step for the evaluation of interfaces such as those that exist in diffusion bonds and thick layered composites. The explicit theoretical relationships between reflection or transmission coefficients, crack density, incident wave frequency and crack size that are validated in this manuscript can be used to interpret ultrasonic waveforms. For example, the percentage of defects in an interface bond can be estimated by observing the relationship between transmission coefficients and the incident wave frequency.

Acknowledgement

This work is partially supported by NSF through Grant MSS-9111339 (LJJ) and grant MSS-9119291 (JQ).

References

1 **Achenbach, J.D.** *Wave Propagation in Elastic Solids* North-Holland Publishing Co., New York (1973)

2 **Ismagilov, F.M., Kravtsov, Y.A. and Lyamshev, L.M.** Enhanced backscattering of acoustic waves reflected from a system of thin randomly oriented plates in a liquid *Akusticheskii Zurnal* (1992) **38** 874–878

3 **Kawahara, J. and Yamashita, T.** Scattering of elastic waves by a fracture zone containing randomly distributed cracks *Pure and Appl Geophys* (1992) **139** 121–144

4 **Rao, N. and Zhu, H.** Scatterer number density estimation using frequency modulated ultrasound pulse *Ultrasonic Symposium Proceedings* (1989) **2** 911–916

5 **Sotiropoulos, D.A. and Achenbach, J.D.** Reflection of ultrasonic waves by an imperfect diffusion *J Nondestruct Eval* (1988) **7** 123–129

6 **Angel, Y.C. and Achenbach, J.D.** Reflection and transmission of elastic waves by a periodic array of cracks *J Appl Mech* (1985) **52** 33–41

7 **Roscoe, R.** The viscosity of suspensions of rigid spheres *Brit J Appl Phys* (1952) **3** 267–269

8 **Auld, B.A.** General electromechanical reciprocity relations applied to the calculations of elastic wave scattering coefficients *Wave Motion* (1979) **1** 3–10

9 **Bruttomesso, D.A., Jacobs, L.J. and Costley, R.D.** Development of an interferometer for acoustic emission testing *J Engineering Mech* (1993) **119** 2303–2316